8-15-2006

# Dissolved Gallium In the Northwest Pacific and the South and Central Atlantic Oceans: Implications for Aeolian Fe Input and a Reconsideration of Profiles

Alan M. Shiller
*University of Southern Mississippi*, alan.shiller@usm.edu

Gautam Raj Bairamadgi
*University of Southern Mississippi*

## Recommended Citation

Shiller, A. M., Bairamadgi, G. R. (2006). Dissolved Gallium In the Northwest Pacific and the South and Central Atlantic Oceans: Implications for Aeolian Fe Input and a Reconsideration of Profiles. *Geochemistry, Geophysics, Geosystems, 7*.
Available at: http://aquila.usm.edu/fac_pubs/2294

Geochemistry Geophysics Geosystems G3
AN ELECTRONIC JOURNAL OF THE EARTH SCIENCES
Published by AGU and the Geochemical Society

*Article*
Volume 7, Number 8
15 August 2006
Q08M09, doi:10.1029/2005GC001118
ISSN: 1525-2027

# Dissolved gallium in the northwest Pacific and the south and central Atlantic Oceans: Implications for aeolian Fe input and a reconsideration of profiles

**Alan M. Shiller and Gautam Raj Bairamadgi**

*Department of Marine Science, University of Southern Mississippi, 1020 Balch Boulevard, Stennis Space Center, Mississippi 39529, USA (alan.shiller@usm.edu)*

[1] The distribution of dissolved gallium, a less-reactive analogue of aluminum, has the potential to reveal information about the averaged dust input to the surface ocean and to complement studies using aluminum as a tracer. New data are presented here on the distribution of dissolved Ga, including six profiles in the south and central Atlantic as well as seven shallow and two deep profiles from the northwest Pacific. The Atlantic data allow for an estimate of Ga in Antarctic Bottom Water (~25–30 pmol kg$^{-1}$) and show reasonably conservative behavior in deep waters. In the northwest Pacific, surface water Ga/Al ratios correlate with chlorophyll concentrations, probably reflecting the biogenic removal of dissolved Al and suggesting a possible means for estimating variation in surface water Al removal times. Also in the northwest Pacific, low surface water Ga in subpolar surface waters suggests low dust input, thereby providing an explanation for the high nutrient–low chlorophyll behavior of this environment. This low Ga subpolar water implies that North Pacific Intermediate Water is low in Ga and thus provides an advective explanation for the intermediate water Ga minimum observed in the temperate North Pacific. Surprisingly, the deepest waters sampled in the North Pacific have Ga concentrations similar to that estimated for circumpolar waters, thus indicating minimal reactivity of Ga in its northward transit in the deep Pacific.

**Components:** 6910 words, 10 figures, 4 tables.

**Keywords:** gallium; lead; aluminum; dust; Atlantic Ocean; northwest Pacific Ocean.

**Index Terms:** 4875 Oceanography: Biological and Chemical: Trace elements (0489); 4801 Oceanography: Biological and Chemical: Aerosols (0305, 4906); 4808 Oceanography: Biological and Chemical: Chemical tracers.

**Received** 14 August 2005; **Revised** 16 May 2006; **Accepted** 9 June 2006; **Published** 15 August 2006.

Shiller, A. M., and G. R. Bairamadgi (2006), Dissolved gallium in the northwest Pacific and the south and central Atlantic Oceans: Implications for aeolian Fe input and a reconsideration of profiles, *Geochem. Geophys. Geosyst.*, *7*, Q08M09, doi:10.1029/2005GC001118.

---

**Theme:** Biogeotracers in the Northwest Pacific Ocean
**Guest Editors:** Michiel Rutgers van der Loeff, William M. Landing, Catherine Jeandel, and Rodney T. Powell

## 1. Introduction

[2] There has been great interest in dust input to the surface ocean in part because this is a major source of the limiting nutrient Fe to the open ocean [e.g., *Martin and Fitzwater*, 1988]. However, the fact that there other sources of dissolved Fe (such as rivers, reducing sediments, and upwelling [e.g., *Fung et al.*, 2000]) as well as the short surface ocean residence time of this element, means that other tracers are required to more fully elucidate the aeolian Fe input to the surface ocean. In particular, dissolved Al distributions have been used in this regard because Al input to the surface ocean is largely dust-derived [e.g., *Orians and Bruland*, 1986]. For instance, the Al-based model of *Measures and Brown* [1996] generates dust flux estimates comparable to other methods. However, the short surface ocean residence time of Al [*Orians and Bruland*, 1986] means that this tracer may offer more of an instantaneous picture of dust input rather than an averaged view. In contrast, gallium, which has a solution chemistry and geochemistry similar to aluminum, has a surface ocean residence time about an order of magnitude greater than Al [*Shiller*, 1998]. The reason for the difference in residence times probably stems from how the difference in hydrolysis constants of the two trivalent ions affects their relative adsorption onto particles as well as the Ga-O bond being longer and more covalent than the Al-O bond, resulting in relative exclusion of Ga from structural sites where it may substitute for Al [*Shiller*, 1988; *Orians and Bruland*, 1988a]. This somewhat longer dissolved Ga residence time may make its surface water distribution more useful in providing an averaged view of aeolian input.

[3] A study of dissolved Ga in the northwest Pacific Ocean is particularly timely for a variety of reasons. The North Pacific subpolar gyre appears to be a high-nutrient-low-chlorophyll (HNLC) region despite the proximity of the Asian dust source and model estimates that indicate high dust deposition in this region [e.g., *Duce et al.*, 1991]. Furthermore, a previous study of Ga in the northeast Pacific suggested additional sources of Ga in the water column and at the sediment-water interface [*Orians and Bruland*, 1988a, 1988b], although those sources were not apparent in an examination of Atlantic Ocean profiles [*Shiller*, 1998]. In this report we provide new data on dissolved Ga distributions in the northwest Pacific Ocean as well as in the south and central Atlantic in an effort to shed light on these issues.

## 2. Methods

[4] Profile and surface water samples analyzed during this study were collected on Intergovernmental Oceanographic Commission (IOC) sponsored cruises in the Atlantic (IOC 1996) and the North Pacific (IOC 2002). The May/June IOC 1996 cruise sampled six stations between Uruguay and Barbados aboard R/V *Knorr* in the tropical and subtropical Atlantic (Figure 1), and the May/June IOC 2002 cruise sampled nine stations between Hawaii and Japan aboard R/V *Melville* in the northwest Pacific (Figure 2).

[5] Sample collection is described in detail elsewhere [*Cutter and Measures*, 1999; *Measures et al.*, 2006] and only the most pertinent details are described here. Vertical profile samples were obtained using contamination-free procedures, including deploying 12 L and 30 L Go-Flo bottles and triggering them with plastic messengers. For surface sampling of trace elements, a torpedo shaped "fish" was deployed and water peristaltically pumped from the fish to a clean lab on the ship through Teflon-lined polyethylene tubing [*Vink et al.*, 2000] where it was pressure-filtered through 0.4 μm Nuclepore polycarbonate membrane filters [*Landing et al.*, 1995]. Samples were finally collected in 500 mL acid-washed HDPE bottles. They were acidified to pH ~ 1.8 in the lab using ultrapure HCl (Seastar Chemicals, Baseline) to resolubilize any metals which might have adsorbed to the walls of the bottles, and then stored in plastic zipper bags. Hydrography and sampling methods for the IOC-96 cruise were described by *Cutter and Measures* [1999] and for the IOC-02 cruise by *Measures et al.* [2006].

[6] A variation of the magnesium hydroxide coprecipitation/isotope dilution/ICP-MS method of *Wu and Boyle* [1997, 1998] was used to determine Ga in the samples. The technique involves addition of clean aqueous ammonia to the acidified seawater sample and precipitating magnesium hydroxide, which in turn, scavenges the trace metals of interest from solution. An enriched isotope spike of known concentration was prepared using purified enriched isotope of 99.8% Ga-71, obtained from Oak Ridge National Laboratories. Initial experiments indicated that various spike equilibration times, ranging from 30 sec. to 24 hr., yielded equivalent results. Trial studies also indicated a significant interference of doubly charged Ba-138 with Ga-69. In order to get rid of as much barium as possible, the precipitate was washed three times with a solution of high purity 0.1% $NH_4OH$. The precipitate was

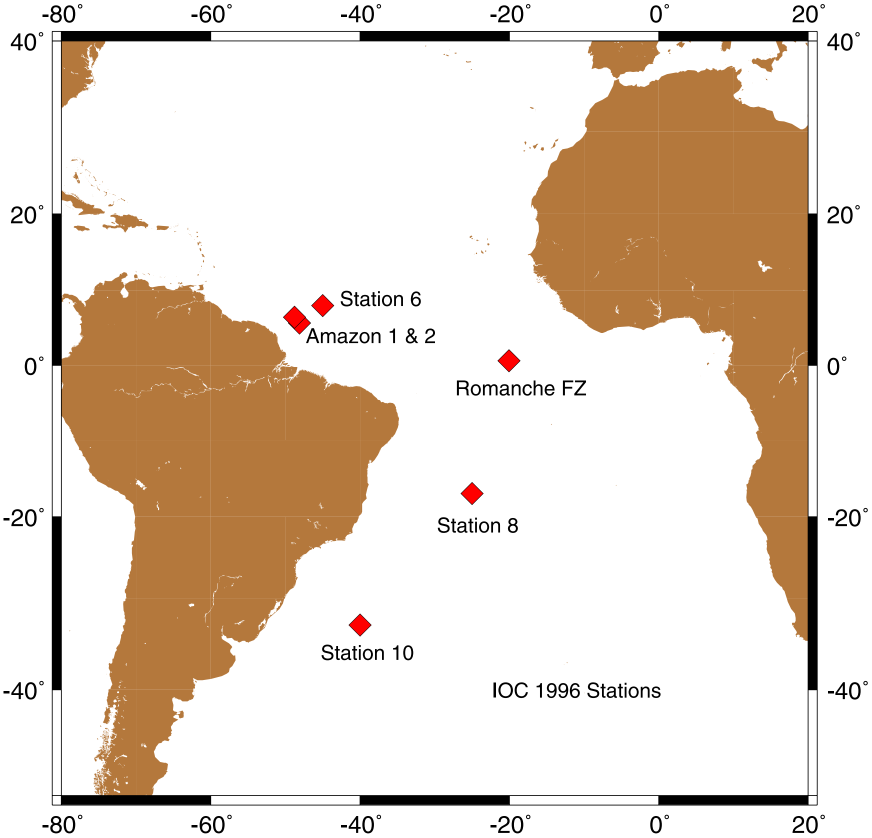

**Figure 1.** Sampling stations for 1996 IOC Contaminants Baseline Survey of the south and central Atlantic Ocean.

then dissolved in 550 μL ultrapure 3% $HNO_3$ (Seastar Chemicals, Baseline) and analyzed in low resolution using a ThermoFinnigan Element 2 High Resolution Inductively Coupled Plasma Mass Spectrometer (HR-ICP-MS). Isotopes monitored on the ICP-MS were Ga-69, Ga-71, and Ba-138. A slight correction for residual Ba was made based on the ratio of responses at masses 69 and 138 to a Ba standard solution. Because the residual salt content varied from sample to sample, it was not possible to matrix-match the Ba correction standard. However, typically, this correction affected the final result by $< 2.5$ pmol $kg^{-1}$; where higher Ba corrections were noted, the sample was reprecipitated and re-analyzed because of concerns about the accuracy of applying the Ba standard correction to samples of high salt content.

[7] Quality control was maintained by analyzing a large-volume seawater Atlantic Ocean surface water sample as well as a standard reference sample (NASS-5) with each run. Precision can be estimated from the replicate analyses of these samples. The average dissolved Ga concentration of the large-volume Atlantic sample was $29.0 \pm 1.9$ pmol $kg^{-1}$ ($n = 83$) and the average concentration of NASS-5 was $6.2 \pm 0.9$ pmol $kg^{-1}$ ($n = 58$). Accuracy was estimated from a spike experiment which gave a Ga recovery of $105 \pm 4\%$. Additionally, a station previously analyzed by column extraction and atomic absorption spectrophotometry (AAS) [*Shiller*, 1998] was redetermined by this new ICP-MS method. Results from the two methods were highly correlated ($r = 0.96$ for $n = 14$), though the new results were typically $2.3 \pm 1.8$ pmol $kg^{-1}$ higher than the previous results. A reduced major axis regression between the two sets of analyses yielded the relation: $Ga(new) = 1.08\ x\ Ga(old) + 1.1$, with an uncertainty of $\pm 0.093$ for the slope and $\pm 1.7$ for the intercept. With such a small disparity between the two sets of analyses, it is difficult to speculate on a cause for the difference, especially given the decade that has passed since the original AAS analyses and our current lack of instrumentation to perform the older analytical method. We also note that north of Hawaii, where our Pacific Ocean surface water data overlap with samples collected by *Orians and Bruland* [1988b], there is good agreement between the two data sets.

[8] Dissolved Pb was determined at the same time as Ga by adding a 92.81% enriched spike of Pb-

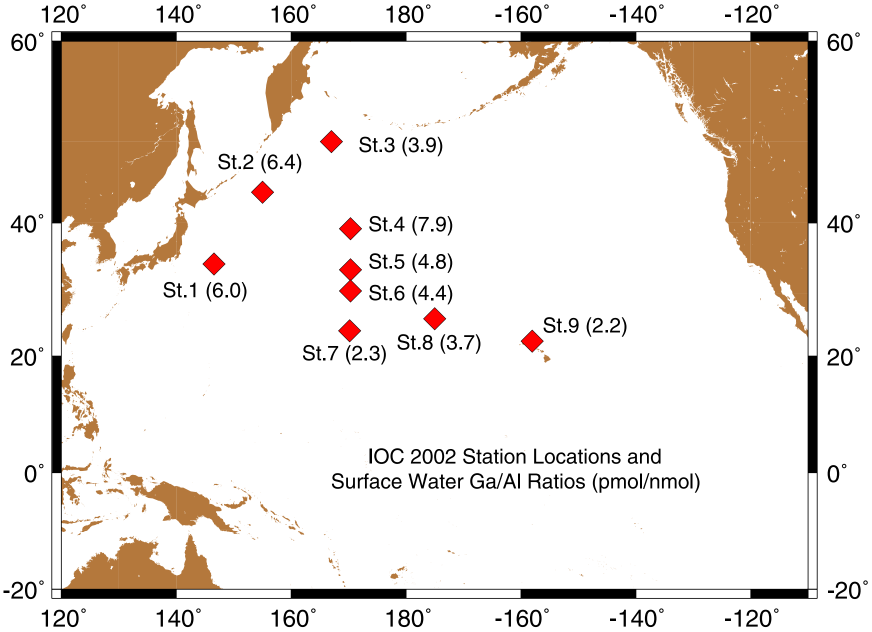

**Figure 2.** Sampling stations for 2002 IOC Contaminants Baseline Survey of the northwest Pacific Ocean. Ga/Al ratios (pmol/nmol) in surface waters are given in parentheses after the station numbers.

207 along with the enriched Ga spike. Repeated analysis of Pb in NASS-5 reference seawater (NRC Canada) yielded a recovery of 89 ± 4%. Results obtained for the Atlantic profiles were similar to those previously published by *Alleman et al.* [2001] and *Ndung'u et al.* [2001].

[9] Contour plots of data were produced using Generic Mapping Tools [*Wessel and Smith*, 1998]. A continuous curvature gridding algorithm was applied to 1-degree averaged data to produce the plots.

## 3. Results and Discussion

### 3.1. South and Central Atlantic

[10] Results from the south and central Atlantic are presented in Tables 1a and 1b. The new profiles from the south and central Atlantic (Figure 3) are consistent with previous work [*Shiller*, 1998]. In general, the profiles show high Ga at the surface, decreasing with depth to a Ga minimum at 700–1000 m and then deep water Ga remains fairly constant.

[11] Two shallow (<500 m) profiles were obtained in the vicinity of the Amazon River plume. While the shallowest samples of these profiles were slightly Ga-enriched compared with samples below, the concentrations are not unusual for this latitude in the Atlantic and thus it is difficult to ascribe any particular effect of the river plume. Note, however, that the salinity of the shallowest, least saline sample (S = 34.7) was not particularly freshened in comparison with the most saline samples of these two profiles (S = 36.6).

[12] The South Atlantic Central Water (SACW), formed by the wintertime convection of surface waters between 35 and 40°S [*Peterson and Whitworth*, 1989] is found from below the mixed layer to the salinity minimum of the Antarctic Intermediate Water (AAIW). A comparison of Ga profiles from the western basin (IOC-96) to the eastern basin (IOC-90) [*Shiller*, 1998] shows about a 4–6 pmol kg$^{-1}$ increase in the SACW in our IOC 1996 profiles.

[13] The Ga minimum seen between ~700 and 970 m (Figure 3) at all stations coincides with waters of the low salinity Antarctic Intermediate Water (AAIW) [*Cutter and Measures*, 1999]. Similar AAIW minimum concentrations have been observed in the south Atlantic for Ga [*Shiller*, 1998] and for Al [*Measures*, 1995]. This trend can be explained by the formation of the AAIW at higher latitudes with lower dust inputs [*Shiller*, 1998; *Measures*, 1995] than the surface waters at these stations. The magnitude of the AAIW Ga minimum is similar in these new profiles to that in the southeast Atlantic [*Shiller*, 1998], suggesting Ga in the AAIW undergoes negligible change through the south Atlantic.

**Table 1a.** Dissolved Gallium in South and Central Atlantic Waters: IOC 1996

| Amazon 1 (5°47.8′N, 47°59.1’W) | | Amazon 2 (6°39.3′N, 48°48.0′W) | | Station Romanche (0°35′S, 20°2′W) | | Station 6 (7°30′N, 25°W) | | Station 8 (17°S, 25°W) | | Station 10 (33°S, 40°W) | |
|---|---|---|---|---|---|---|---|---|---|---|---|
| Depth, m | Ga, pmol/kg | Depth, m | Ga, pmol/kg | Depth, m | Ga, pmol/kg | Depth, m | Ga, pmol/kg | Depth, m | Ga, pmol/kg | Depth, m | Ga, pmol/kg |
| 5 | 32.4 | 7 | 31.7 | 15 | 25.7 | 20 | 33.6 | 15 | 21.0 | 15 | 21.4 |
| 15 | 29.7 | 20 | 28.0 | 40 | 23.9 | 40 | 32.2 | 50 | 27.6 | 60 | 27.1 |
| 40 | 26.1 | 32 | 26.7 | 60 | 20.9 | 63 | 36.2 | 90 | 19.9 | 100 | 21.8 |
| 60 | 27.1 | 48 | 25.7 | 80 | 19.0 | 83 | 34.3 | 110 | 20.3 | 120 | 25.3 |
| 90 | 21.8 | 69 | 26.1 | 110 | 17.2 | 94 | 37.9 | 140 | 15.8 | 150 | 21.3 |
| 120 | 25.7 | 75 | 27.7 | 140 | 17.7 | 110 | 33.4 | 170 | 19.1 | 200 | 25.3 |
| 150 | 26.2 | 115 | 23.6 | 180 | 17.0 | 150 | 28.4 | 220 | 18.3 | 230 | 19.9 |
| 200 | 25.6 | 150 | 20.1 | 200 | 15.3 | 200 | 21.4 | 270 | 19.9 | 270 | 23.9 |
| 240 | 18.7 | 200 | 14.7 | 220 | 16.9 | 260 | 20.4 | 350 | 15.8 | 330 | 18.0 |
| 300 | 16.1 | 300 | 11.4 | 350 | 15.2 | 300 | 17.9 | 500 | 6.4 | 400 | 22.3 |
| 400 | 15.1 | 400 | 11.8 | 500 | 11.7 | 400 | 19.1 | 600 | 6.3 | 500 | 11.6 |
| 500 | 13.9 | 500 | 12.1 | 600 | 10.8 | 500 | 17.1 | 750 | 10.5 | 700 | 12.7 |
| | | | | 750 | 10.8 | 600 | 13.0 | 850 | 14.8 | 900 | 12.3 |
| | | | | 850 | 13.6 | 700 | 13.2 | 1000 | 19.8 | 1050 | 12.5 |
| | | | | 1300 | 22.9 | 800 | 13.3 | 1150 | 14.8 | 1400 | 16.2 |
| | | | | 1500 | 28.2 | 900 | 15.0 | 1320 | 24.6 | 1550 | 23.1 |
| | | | | 1650 | 29.9 | 1000 | 16.9 | 1500 | 32.1 | 1900 | 25.5 |
| | | | | 1800 | 30.9 | 1200 | 22.6 | 1800 | 36.6 | 2100 | 34.1 |
| | | | | 1950 | 30.9 | 1400 | 34.8 | 2000 | 34.0 | 2250 | 33.4 |
| | | | | 2100 | 31.4 | 1550 | 37.3 | 2600 | 38.9 | 2550 | 37.4 |
| | | | | 2500 | 31.3 | 1750 | 37.5 | 2800 | 39.2 | 2700 | 37.6 |
| | | | | 2670 | 31.8 | 1950 | 36.7 | 3015 | 34.9 | 3100 | 32.7 |
| | | | | 2920 | 30.8 | 2250 | 40.0 | 3400 | 36.7 | 3450 | 33.7 |
| | | | | 3420 | 33.8 | 2550 | 37.9 | 4115 | 35.5 | 3695 | 40.0 |
| | | | | 3920 | 33.8 | 2800 | 33.0 | 4415 | 27.1 | 3780 | 31.6 |
| | | | | 4170 | 30.7 | 3000 | 38.2 | 4715 | 29.9 | 4350 | 30.9 |
| | | | | 4620 | 28.6 | 3200 | 34.2 | 5015 | 26.4 | | |
| | | | | 5070 | 29.0 | 3600 | 34.9 | 5065 | 25.9 | | |
| | | | | 5170 | 27.7 | 4000 | 37.7 | 5155 | 26.7 | | |
| | | | | 5220 | 27.8 | 4500 | 37.3 | | | | |
| | | | | | | 4550 | 36.0 | | | | |

[14] Waters between ~1600 to ~4200 m are from the North Atlantic Deep Water (NADW), which is divided into an upper NADW (1600–3000 m) with decreasing silicate and increasing salinity and a lower NADW (3000–4200 m) with uniform silicate and salinity [*Cutter and Measures*, 1999]. In general, dissolved Ga in this depth range was somewhat higher (~5–10 pmol $kg^{-1}$) in the new western basin profiles than in the previous [*Shiller*, 1998] eastern basin profiles. However, dissolved Si was higher in the eastern basin profiles, suggesting a greater admixture of Antarctic Bottom Water, which is high in Si and low in Ga.

[15] Stations 8 and Romanche had a bottom layer with significantly lower Ga than the waters above. These were the two stations where we obtained samples deep enough to sample the low salinity, low temperature, and high silicate water characteristic of AABW [*Cutter and Measures*, 1999]. The lower Ga content in the AABW is likely due to its Southern Ocean origin where aeolian inputs are expected to be minimal. A similar decrease in concentrations in the AABW was reported previously for Ga [*Shiller*, 1998] and Al [*Measures*, 1995]. A plot of Ga versus Si for the deep (>2500 m) waters of these south and central Atlantic stations (Figure 4), indicates that Ga in the high Si (~120 μmol $kg^{-1}$) AABW end-member is ~25–30 pmol $kg^{-1}$, somewhat higher than previously estimated [*Shiller*, 1998].

[16] Although dissolved Ga in AABW is lower than in NADW, it is still comparatively high. Thus one might ask why Ga in AABW is not more similar in concentration to AAIW, both of which originate in low dust input southern hemisphere waters. A similar question can be raised for Al, which shows low concentrations (relative to NADW) in both AAIW and AABW but with AABW concentrations roughly twice those of AAIW [*Measures and Edmond*, 1990; *Measures*, 1995]. *Measures and Edmond* [1990] suggested an

**Table 1b.** IOC 1996 (Continued)

| Surface Water Data | | |
|---|---|---|
| Latitude | Longitude | Ga, pmol/kg |
| −33.82 | −46.30 | 29.60 |
| −33.70 | −45.22 | 29.62 |
| −33.26 | −41.83 | 30.77 |
| −33.07 | −40.45 | 30.67 |
| −30.23 | −38.28 | 26.14 |
| −28.90 | −36.95 | 29.51 |
| −26.80 | −33.76 | 29.58 |
| −26.15 | −34.07 | 28.59 |
| −25.38 | −33.33 | 28.79 |
| −17.25 | −25.25 | 27.30 |
| −14.12 | −24.10 | 31.24 |
| −13.45 | −23.89 | 29.37 |
| −11.09 | −23.18 | 23.59 |
| −10.41 | −23.01 | 24.75 |
| −9.77 | −22.82 | 25.10 |
| −7.15 | −22.00 | 25.53 |
| −6.20 | −21.73 | 27.25 |
| −5.30 | −21.44 | 24.37 |
| −3.05 | −20.77 | 24.87 |
| −2.38 | −20.54 | 25.49 |
| −0.88 | −20.12 | 26.10 |
| 2.07 | −21.13 | 27.51 |
| 2.70 | −21.60 | 26.31 |
| 3.56 | −21.96 | 26.75 |
| 4.56 | −22.79 | 28.16 |
| 5.15 | −26.84 | 28.36 |
| 5.27 | −27.84 | 28.20 |
| 5.81 | −30.90 | 36.59 |
| 6.00 | −31.98 | 35.28 |
| 6.12 | −46.35 | 41.68 |
| 6.47 | −35.10 | 35.95 |
| 6.57 | −46.07 | 36.90 |
| 6.62 | −36.19 | 36.29 |
| 6.72 | −48.88 | 35.12 |
| 6.79 | −37.30 | 36.94 |
| 6.80 | −48.98 | 42.68 |
| 7.28 | −40.15 | 36.84 |
| 7.34 | −40.82 | 27.66 |
| 7.51 | −41.94 | 27.37 |
| 7.92 | −44.65 | 28.75 |

Al-enriched shelf water component elevated AABW Al concentrations above those of the AAIW. *Hall and Measures* [1998] argued that Al enrichment of NADW originated from sediment-water interface remobilization of aeolian Al that had been rapidly scavenged from surface waters. In contrast, *Shiller* [1998] preferred *Moran and Moore*'s [1991] sediment resuspension mechanism for Ga enrichment of NADW. *Lacan and Jeandel* [2004] similarly concluded that margin/seawater interactions affect rare earth element and Nd isotope compositions in certain NADW source waters. While the present data set does not allow us to resolve the specific enrichment mechanisms, we do note that the available data indicates a Ga/Al ratio for NADW of ~2 pmol/nmol contrasting with ~4 pmol/nmol for AABW. These differing ratios suggest the possibility of different enrichment mechanisms for these two deep water masses.

[17] Dissolved Ga in the surface waters from the south Atlantic cruise (as combined with previous results from *Shiller* [1998]; Figure 5) show the highest values in the Intertropical Convergence Zone (ITCZ) north of the equator, as would be expected from persistent African dust input. Additionally, high values are seen at the southern part of 2002 Uruguay-to-Barbados transect. This corresponds to the Brazil Current which also has elevated dissolved Al [*Vink and Measures*, 2001]. Because waters in the South Equatorial Current appear to have lower Ga, this is unlikely to be an advective feature. Possibly, westerly winds from South America may supply dust to these waters.

## 3.2. Northwest Pacific

[18] Results from the northwest Pacific are presented in Tables 2a and 2b. Dissolved Ga in surface waters of the northwest Pacific ranged from 5 to 21 pmol $kg^{-1}$ with the lowest values in the subpolar gyre and the highest values near Japan (Figure 6). Combined with the previous data from *Orians and Bruland* [1988b] (open circles in Figure 6) the North Pacific shows an east-west gradient in surface water Ga concentrations consistent with lower aeolian input further away from the Asian continent. Consistently low Ga in the subpolar HNLC region suggests that the low Al and Fe observed in these waters during this cruise [*Measures et al.*, 2005; *Brown et al.*, 2005] reflect a persistent lack of dust input to these waters rather than a temporary feature. This is a surprising finding considering that the aerosol index produced by the total ozone mapping spectrometer (TOMS) does show dust storms passing over this region (e.g., see aerosol index maps for the periods March 20–25 and April 20–25, 2002 viewable at http://toms.gsfc.nasa.gov/aerosols/aerosols_v8.html). Nonetheless, the low dust input implied by the Ga data does provide an explanation for why the northwest Pacific is an HNLC region.

[19] As mentioned by *Measures et al.* [2005], other work indicates that Asian surface air can be entrained into the troposphere above the marine boundary layer [e.g., *Hannan et al.*, 2003] and this can provide a mechanism by which Asian dust may avoid deposition close to the Asian continent. Indeed, *Liu et al.* [2003] note that boundary layer outflow to the western Pacific tends not to be influenced by Asian biomass burning. And *Cooper*

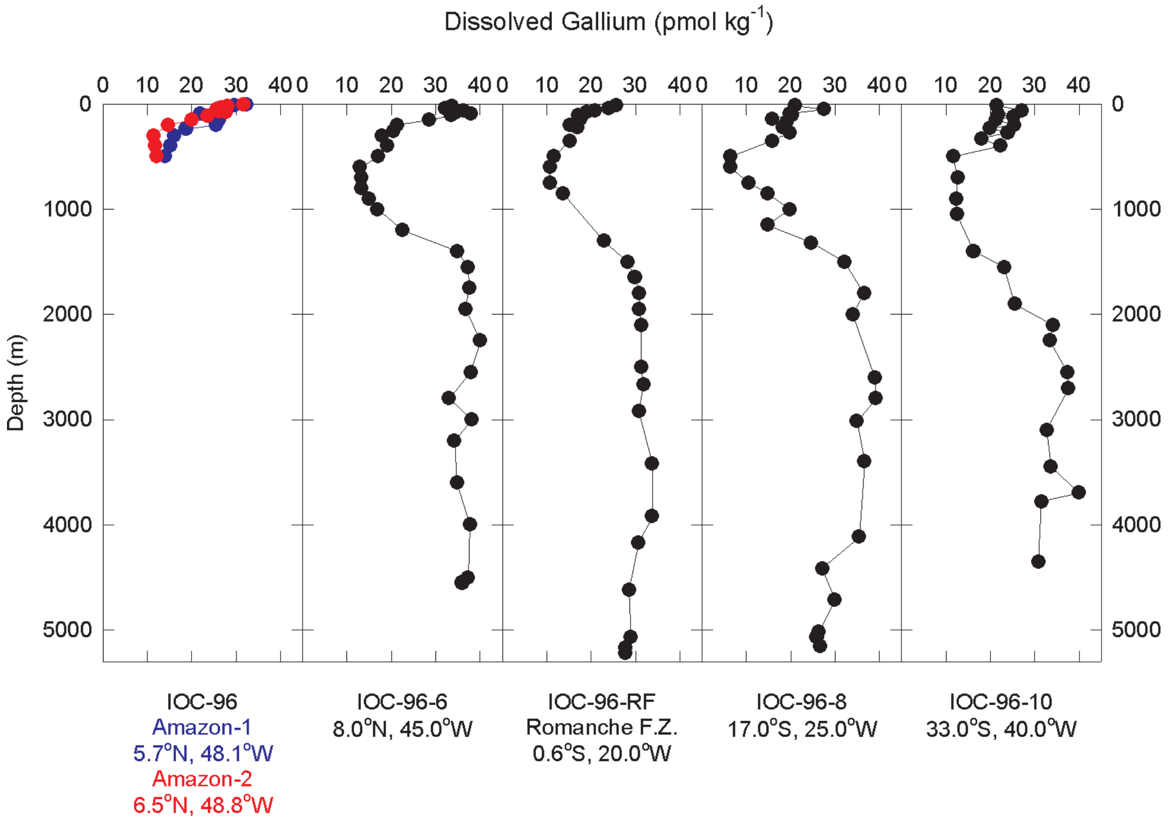

**Figure 3.** Dissolved gallium profiles in the south and central Atlantic Ocean.

*et al.* [2004], during the time of the IOC 2002 cruise, observed entrainment of polluted Asian air into the "warm conveyor belt" and transport across the North Pacific to the west coast of North America.

[20] In the surface waters, we have also examined the variation in the dissolved Ga/Al ratio (Figure 2). There is a surprisingly large variation in this ratio with little obvious relationship to location. However, we do observe a relationship between the Ga/Al ratio and chlorophyll *a* concentrations (Figure 7). This relationship implies that greater biomass enhances biogenic scavenging removal of Al [*Measures et al.*, 1984; *Moran and Moore*, 1988; *Hydes*, 1989] relative to Ga, thereby increasing the Ga/Al ratio. If indeed the Ga removal rate is comparatively insensitive to biomass, then the fourfold variation in the surface water Ga/Al ratio in the northwest Pacific indicates at least a fourfold variation in the Al scavenging residence time. If true, this also suggests the use Ga or chlorophyll data to compensate for residence time variations in Al-based estimates of dust deposition to the surface ocean [e.g., *Measures et al.*, 2005]. One might do this, for instance, by assuming that the lowest value of the Ga/Al ratio corresponds to a 5-year dissolved Al residence time in oligotrophic waters [*Orians and Bruland*, 1986; *Measures and Brown*, 1996] and that the Ga/Al ratio is inversely proportional to the Al residence time. Use of the Ga/Al-chlorophyll relationship could allow this correction to be extended to other regions where Ga data have not been obtained. Clearly, though, this approach is limited both by our knowledge of the surface ocean residence time of Al as well as the mechanisms controlling surface water Ga removal.

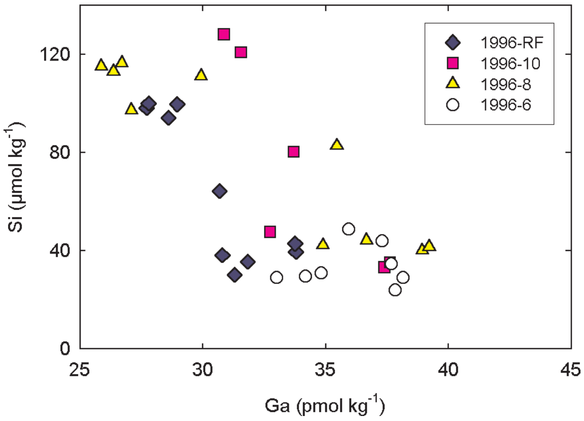

**Figure 4.** Dissolved gallium versus silica in deep (>2500 m) waters of the south and central Atlantic.

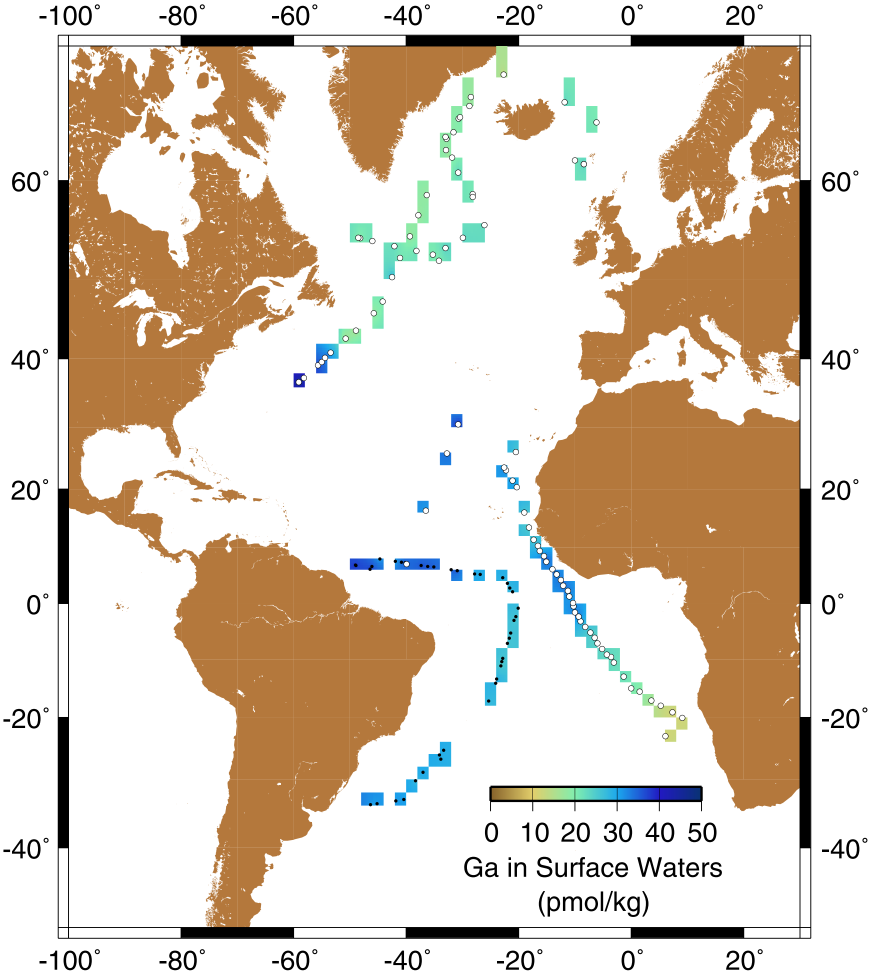

**Figure 5.** Dissolved gallium in surface waters of the Atlantic Ocean. Closed circles: new data from IOC 1996; open circles: data from *Shiller* [1998].

[21] A comparison of the dissolved Pb and Ga data for these surface waters is also instructive (Figure 8). Three distinct end-members are observed in this diagram: (1) waters near Japan which have the highest Pb and Ga, (2) subpolar waters which have moderate Pb and low Ga, and (3) subtropical gyre waters having comparatively low Pb and moderate Ga. That Pb is reasonably high in subpolar waters suggests either that some aerosols from Asia are deposited in these waters (i.e., the Pb is indicative of an Asian pollution source) or there is another non-aeolian source of Pb to the subpolar gyre. While these data do not allow for a distinction between these two possibilities, it seems hard to reconcile aeolian pollutant Pb input with the lack of aeolian Ga, Al, and Fe input. In any event, the Pb data allow us to partially address the issue of possible anthropogenic Ga input to the surface ocean [*Shiller*, 1988]. One would presume that the surface waters near Japan having the highest Pb and also the highest measured dissolved Ag [*Ranville and Flegal*, 2005], would be the most contaminated with anthropogenic Ga from coal combustion. In comparing the high Pb-high Ga waters near Japan with those in the central part of the subtropical gyre (Figure 8), a simple mixing approach (ignoring differences in removal for the two elements) would suggest a 5–10 pmol $kg^{-1}$ anthropogenic Ga contribution. Likewise, if all the Pb in the subpolar gyre is anthropogenic, then a similar assumption would indicate 5–8 pmol $kg^{-1}$ anthropogenic Ga. These are obviously maximum estimates and suggest that anthropogenic Ga is probably a minor fraction of the total in most, if not all, areas of the ocean.

[22] Our vertical profiles of dissolved Ga in the northwest Pacific (Figure 9) show similarities and differences compared to the *Orians and Bruland* [1988a, 1988b] profiles from the northeast Pacific. Both of our deep water stations show a Ga minimum of about 10 pmol $kg^{-1}$ at ∼1000 m seen previously by *Orians and Bruland* [1988a, 1988b].

**Table 2a.** Dissolved Gallium in Northwest Pacific Waters: IOC 2002

| Station 1 (34°28′N, 146°59.2′E) | | Station 2 (44°N, 155°E) | | Station 3 (50°N, 167°E) | |
|---|---|---|---|---|---|
| Depth, m | Ga, pmol/kg | Depth, m | Ga, pmol/kg | Depth, m | Ga, pmol/kg |
| 15 | 19.8 | 20 | 5.7 | 20 | 3.6 |
| 40 | 19.0 | 60 | 5.7 | 60 | 3.0 |
| 80 | 20.1 | 80 | 6.9 | 80 | 4.0 |
| 200 | 21.6 | 100 | 6.7 | 100 | 4.4 |
| 300 | 16.8 | 150 | 5.1 | 150 | 4.2 |
| 475 | 20.7 | 230 | 6.3 | 250 | 5.4 |
| 550 | 13.9 | 300 | 5.1 | 300 | 7.2 |
| 675 | 12.5 | 600 | 14.3 | 500 | 7.8 |
| 1200 | 13.8 | 900 | 9.1 | 700 | 9.2 |
| 1400 | 13.2 | 1500 | 13.5 | 900 | 9.6 |
| | | 2000 | 14.5 | 1200 | 9.7 |
| | | 2500 | 18.9 | 1500 | 10.1 |
| | | 4000 | 18.5 | | |
| | | 4500 | 29.7 | | |

| Station 4 (39°21.5′N, 170°34.5′E) | | Station 5 (33°45.9′N, 170°35′E) | | Station 6 (30°30′N, 170°34.5′E) | |
|---|---|---|---|---|---|
| Depth, m | Ga, pmol/kg | Depth, m | Ga, pmol/kg | Depth, m | Ga, pmol/kg |
| 20 | 15.4 | 20 | 17.7 | 20 | 17.5 |
| 60 | 16.7 | 60 | 18.3 | 60 | 17.8 |
| 80 | 14.9 | 80 | 19.2 | 150 | 18.0 |
| 120 | 14.9 | 120 | 19.6 | 200 | 18.1 |
| 175 | 13.5 | 175 | 15.3 | 250 | 17.0 |
| 250 | 12.0 | 250 | 15.7 | 300 | 16.0 |
| 300 | 12.0 | 300 | 16.0 | 500 | 14.6 |
| 500 | 10.6 | 500 | 15.5 | 650 | 11.8 |
| 900 | 10.4 | 900 | 12.7 | 900 | 9.7 |
| 1200 | 10.8 | 1200 | 7.6 | 1200 | 10.9 |
| 1500 | 10.6 | 1500 | 9.3 | 1500 | 12.3 |

| Station 7 (24°15′N, 170°20′E) | | Station 8 (26°N, 175°W) | | Station 9 (22°45′N, 158°W) | |
|---|---|---|---|---|---|
| Depth, m | Ga, pmol/kg | Depth, m | Ga, pmol/kg | Depth, m | Ga, pmol/kg |
| 20 | 14.0 | 20 | 15.0 | 20 | 13.0 |
| 60 | 15.0 | 40 | 16.2 | 60 | 14.1 |
| 100 | 13.4 | 80 | 15.0 | 80 | 12.6 |
| 150 | 15.5 | 100 | 16.6 | 100 | 13.7 |
| 200 | 18.2 | 170 | 16.9 | 150 | 13.6 |
| 250 | 17.1 | 250 | 16.8 | 200 | 12.0 |
| | | 300 | 17.3 | 300 | 13.1 |
| | | 500 | 18.0 | 500 | 10.9 |
| | | 700 | 10.1 | 775 | 8.0 |
| | | 900 | 11.8 | 1750 | 15.8 |
| | | 1200 | 12.5 | 2500 | 20.4 |
| | | 1500 | 10.5 | 3000 | 22.1 |
| | | | | 3500 | 25.9 |
| | | | | 4500 | 28.0 |

Also, deep water Ga increased steadily from the Ga minimum to the bottom, similar to the observations of *Orians and Bruland* [1988a, 1988b].

[23] *Orians and Bruland* [1988b] consistently observed a Ga minimum of 4–10 pmol $kg^{-1}$ in the 500–1000 m depth range in the NE Pacific which they suggested most likely resulted from mid-depth scavenging of Ga. Our two deep stations also show a similar mid-depth Ga minimum and all of our profiles show low (~10 pmol $kg^{-1}$) Ga at this depth range (Figure 9a). In the south Atlantic, however, a similar feature appears to be related to the AAIW (see above and *Shiller* [1998]) and we note that in the Pacific this is the depth range of the North Pacific Intermediate Water (NPIW). Formation of NPIW is still a subject of some uncertainty,

**Table 2b.** IOC 2002 (Continued)

| Surface Water Data | | |
|---|---|---|
| Latitude | Longitude | Ga, pmol/kg |
| 22.42 | −160.678 | 14.8 |
| 22.68 | −158.234 | 12.8 |
| 23.18 | −163.146 | 14.2 |
| 23.62 | −164.372 | 15.0 |
| 23.84 | −155.736 | 14.2 |
| 23.99 | −165.327 | 14.4 |
| 24.39 | −154.609 | 12.9 |
| 24.40 | 170.336 | 14.4 |
| 24.56 | −153.563 | 13.8 |
| 24.76 | 172.765 | 14.4 |
| 24.82 | −167.801 | 12.6 |
| 24.86 | −153.625 | 13.5 |
| 25.02 | 173.983 | 16.1 |
| 25.19 | −168.558 | 14.3 |
| 25.20 | −169.974 | 15.7 |
| 25.27 | 175.197 | 15.8 |
| 25.66 | −172.519 | 14.1 |
| 25.83 | 177.863 | 15.5 |
| 25.85 | −173.871 | 13.3 |
| 26.03 | −151.154 | 11.5 |
| 26.11 | 179.205 | 15.5 |
| 26.18 | −175.299 | 10.7 |
| 26.40 | −179.401 | 13.9 |
| 26.41 | 170.414 | 16.7 |
| 26.65 | −152.060 | 13.9 |
| 26.88 | −150.137 | 13.6 |
| 26.97 | −176.658 | 15.1 |
| 27.69 | −151.299 | 14.8 |
| 27.73 | −150.142 | 14.7 |
| 28.66 | −150.602 | 14.7 |
| 30.78 | 170.577 | 18.9 |
| 32.92 | 170.577 | 18.3 |
| 35.95 | 170.577 | 18.5 |
| 37.10 | 170.577 | 18.6 |
| 39.58 | 170.577 | 15.4 |
| 29.99 | 170.556 | 19.8 |
| 28.85 | 170.510 | 16.3 |
| 39.76 | 147.940 | 15.8 |
| 34.73 | 147.163 | 20.2 |
| 34.00 | 146.577 | 19.1 |
| 32.84 | 145.670 | 19.6 |
| 38.27 | 145.558 | 15.6 |
| 31.89 | 144.936 | 20.8 |
| 37.66 | 144.565 | 17.1 |
| 34.61 | 144.144 | 19.1 |
| 29.00 | 142.742 | 18.8 |
| 34.53 | 142.713 | 17.7 |
| 34.80 | 141.427 | 17.5 |
| 35.36 | 141.046 | 19.8 |
| 40.44 | 149.034 | 14.8 |
| 41.11 | 150.138 | 18.5 |
| 42.09 | 170.577 | 14.5 |
| 42.59 | 152.606 | 7.8 |
| 43.47 | 170.577 | 13.4 |
| 43.78 | 154.627 | 6.0 |
| 44.00 | 155.000 | 7.2 |
| 44.51 | 155.973 | 6.9 |
| 44.68 | 170.577 | 8.1 |
| 45.17 | 157.244 | 6.7 |
| 45.88 | 158.611 | 6.3 |

**Table 2b.** (continued)

| Surface Water Data | | |
|---|---|---|
| Latitude | Longitude | Ga, pmol/kg |
| 47.17 | 170.577 | 5.7 |
| 47.29 | 161.419 | 5.0 |
| 48.03 | 162.908 | 6.2 |
| 48.35 | 170.577 | 6.8 |
| 48.70 | 164.287 | 5.0 |
| 49.54 | 170.577 | 5.0 |

but appears to involve cabbeling of Okhotsk Intermediate Water (OIW) and Gulf of Alaska Intermediate Water (GAIW) when they mix with Kuroshio Water [e.g., *You*, 2005]. Although waters in the Okhotsk Sea have not been sampled for Ga, our northernmost profile (Station 3) along with our surface water data and the high latitude data of *Orians and Bruland* [1988b] all suggest that OIW along with GAIW are likely to be low in Ga. The higher Ga in subtropical surface waters as well as Pacific Deep Water (PDW) thus makes the NPIW appear as a Ga minimum.

[24] *Orians and Bruland* [1988b] also consistently observed a Ga maximum in the NE Pacific at 150–300 m, which they attributed to reversible exchange processes in preference to an advective explanation. *Shiller* [1998] found little evidence for such a maximum in the Atlantic Ocean and our NW Pacific profiles here show only a minimal hint of this maximum. It would thus seem that an advective rather than chemical origin of this maximum is likely. In the North Pacific there appear to be at least two different thermostads in the upper waters [*Suga et al.*, 1997] and these mode waters may well have Ga concentrations characteristic of their formation areas and distinct from overlying near-surface waters affected by local atmospheric inputs.

[25] Figure 10 presents a Ga-salinity plot for the deep waters. For the 1996 south Atlantic stations we show all data below 2500 m. For our deep Pacific profiles, as well as *Orians and Bruland*'s [1998b] VERTEX IV profile (28.25°N, 155°W, near Station 9), we show all data below 750 m. The oval on the plot was based on our estimate of the composition of AABW (Figure 4). This oval also encompasses the deepest samples from the North Pacific profiles. That is, Ga content of the deepest Pacific Deep Water (PDW) looks similar to the Ga content of the circumpolar source waters. This would imply that any net input of Ga from the sediments is minimal otherwise one would expect

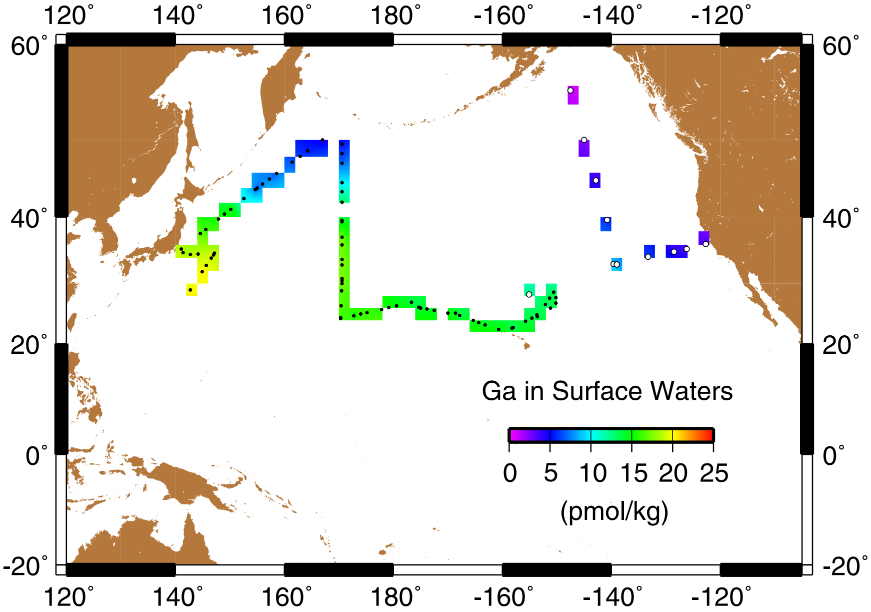

**Figure 6.** Dissolved gallium in surface waters of the northwest Pacific Ocean. Closed circles: new data from IOC 2002; open circles: data from *Orians and Bruland* [1988b].

Ga in the PDW to be significantly elevated from circumpolar concentrations.

[26] The low salinity part of Figure 10 shows the mixing trend between NPIW and PDW. The curvature in this plot implies either Ga scavenging in the water column or else more than two end-members. We note that the break in this curve occurs in the salinity range of ~34.5–34.6 (depth >~1200 m), and that potential temperature-salinity plots in this part of the ocean only become reasonably linear below this depth range. In other words, it is difficult to discern non-conservative behavior of Ga in the PDW. The implication of these observations is that the deep ocean residence time of Ga may be significantly longer than the 750 years estimated by *Orians and Bruland* [1988a] who utilized a scavenging removal model.

## 4. Summary and Conclusions

[27] New data on dissolved Ga in the Atlantic and North Pacific are in general agreement with previously reported oceanic Ga data. New Atlantic surface water data are similar to previous data and show high Ga concentrations beneath the ITCZ, as expected for an element with significant aeolian input. In the south Atlantic, little difference

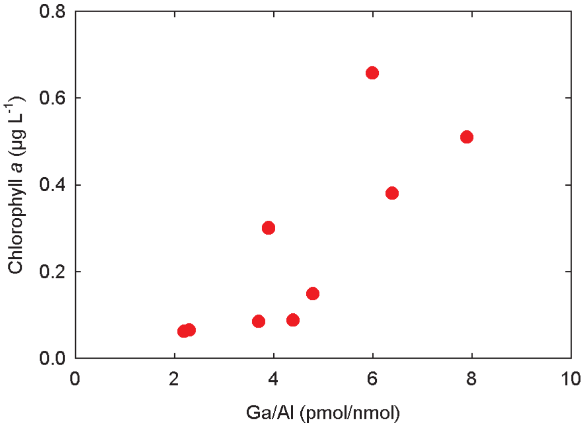

**Figure 7.** Dissolved gallium/aluminum ratio versus chlorophyll *a* in surface waters of the northwest Pacific Ocean.

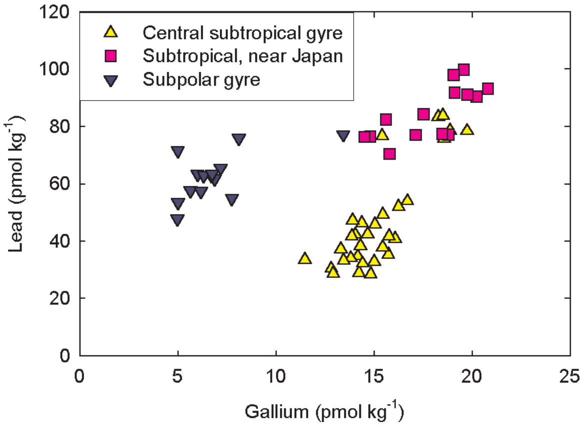

**Figure 8.** Dissolved gallium versus lead for surface waters of the northwest Pacific Ocean.

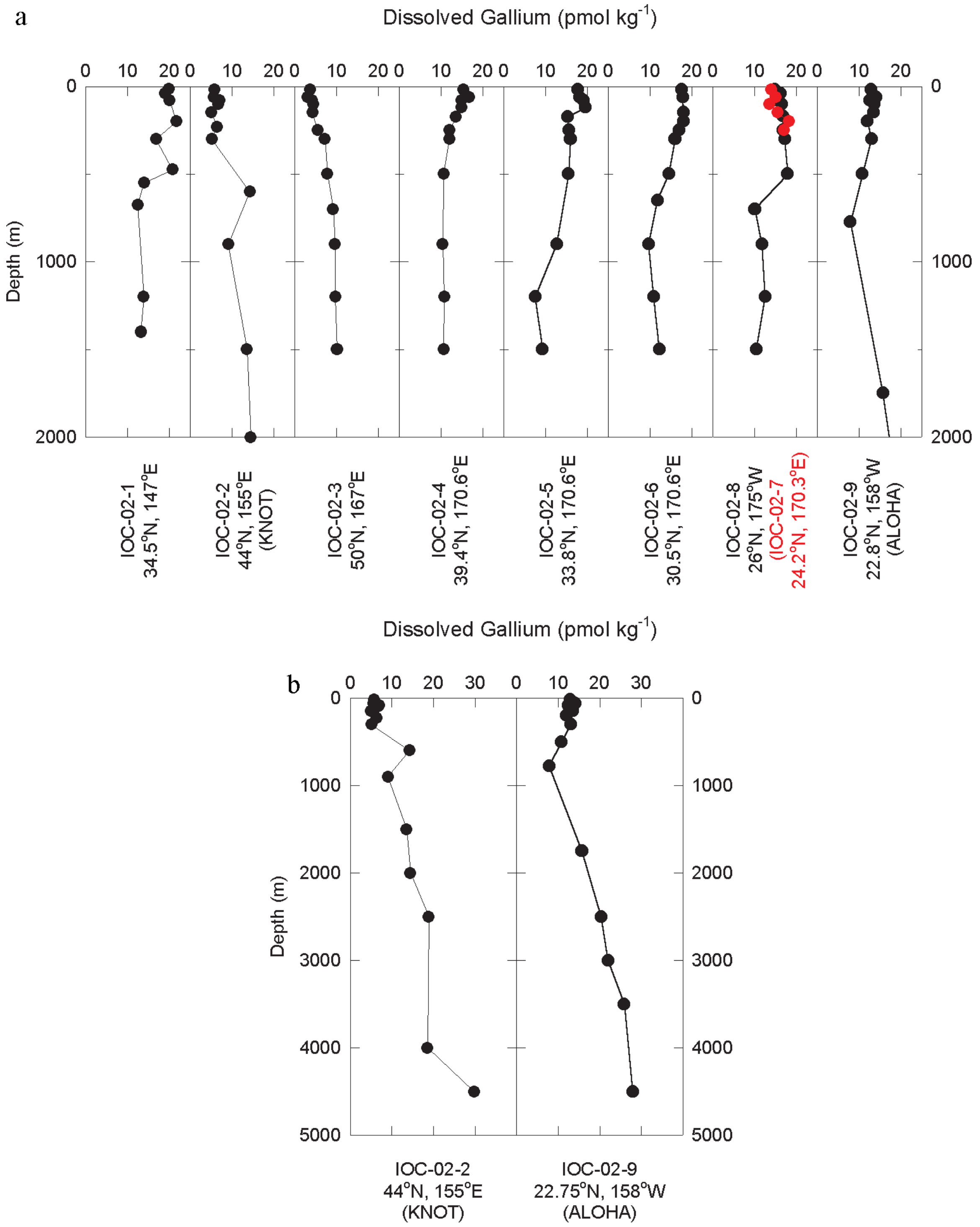

**Figure 9.** Dissolved gallium profiles in the northwest Pacific Ocean. (a) Intermediate depth range for all profiles. (b) Deep profiles at Stations 2 and 9.

in SACW or AAIW is noted between the eastern and western basins. A Si-Ga plot allows for the estimation of Ga in AABW (~25–30 pmol kg$^{-1}$), somewhat higher than previously estimated, though lower than NADW. Deep waters do show higher Ga in our western south Atlantic profiles than in the previous eastern south Atlantic profiles; however, the eastern profiles have higher Si indicating a greater percentage of AABW.

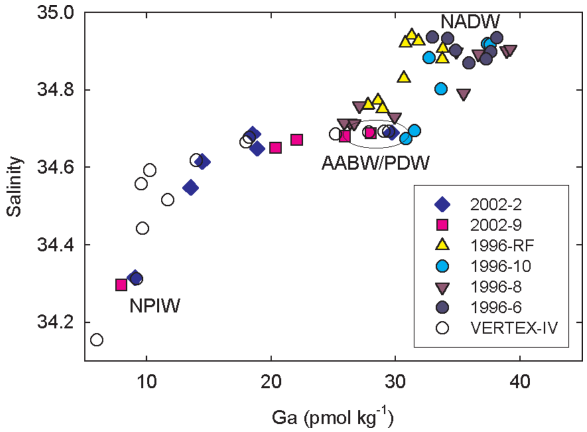

**Figure 10.** Dissolved gallium versus salinity. Plotted data include samples from >2500 m in the south Atlantic and >750 m in the North Pacific (including VERTEX IV profile from *Orians and Bruland* [1988a, 1988b]).

[28] In the northwest Pacific, low Ga in surface waters of the subpolar gyre indicates low dust input and thus provides an explanation for the HNLC region there. Ga/Al ratios in northwest Pacific surface waters show no obvious spatial trend, but do correlate with chlorophyll concentrations. This suggests enhanced biological removal of the more reactive Al relative to Ga and also offers a possible means for adjusting Al-based dust deposition models to account for varying surface water Al residence times. The surface water data also show that the highest surface water Ga concentrations in the northwest Pacific are observed where there is the highest Pb, suggesting at least a small, but observable anthropogenic Ga input.

[29] A consideration of Ga profiles in the northwest Pacific indicates that the previously reported intermediate water Ga minimum is probably an advective feature characteristic of low-dust-input formation waters of the NPIW. In contrast to observations in the northeast Pacific, we do not observe a subsurface Ga maximum, suggesting that the northeast Pacific phenomenon is advective in origin. Likewise, we see little difference between deep North Pacific Ga concentrations and the Ga concentration inferred for circumpolar waters. Thus Ga in the deep ocean is probably less reactive and has a longer residence time than previously thought.

## Acknowledgments

[30] The authors would like to thank the U.S. NSF for funding this work (OCE0137359); C. Measures (UH), G. Cutter (ODU) and W. Landing (FSU) for the invitation to participate in the IOC cruises and for access to ancillary cruise data. J. Yuan (USM) participated in both cruises, helping to collect these samples; W. Landing graciously demonstrated the MagIC method; C. Measures provided the Al data used in Figure 7. Lyndsie Gross (USM) was “instrumental” in operating the ICP-MS and preparing materials. We thank K. Orians, C. Jeandel, and another anonymous reviewer for comments leading to a better manuscript.

## References

Alleman, L. Y., T. M. Church, P. Ganguli, A. J. Veron, B. Hamelin, and A. R. Flegal (2001), Role of oceanic circulation on contaminant lead distribution in the South Atlantic, *Deep Sea Res., Part II*, *48*, 2855–2876.

Brown, M. T., W. M. Landing, and C. I. Measures (2005), Dissolved and particulate Fe in the western and central North Pacific: Results from the 2002 IOC cruise, *Geochem. Geophys. Geosyst.*, *6*, Q10001, doi:10.1029/2004GC000893.

Cooper, O. R., et al. (2004), A case study of transpacific warm conveyor belt transport: Influence of merging airstreams on trace gas import to North America, *J. Geophys. Res.*, *109*, D23S08, doi:10.1029/2003JD003624.

Cutter, G. A., and C. I. Measures (1999), The 1996 IOC contaminant baseline survey in the Atlantic Ocean from 33S to 10N: Introduction, sampling protocols, and hydrographic data, *Deep Sea Res., Part II*, *46*, 867–884.

Duce, R. A., et al. (1991), The atmospheric input of trace species to the World Ocean, *Global Biogeochem. Cycles*, *5*, 193–259.

Fung, I. Y., S. K. Meyn, I. Tegen, S. C. Doney, J. G. John, and J. K. B. Bishop (2000), Iron supply and demand in the upper ocean, *Global Biogeochem. Cycles*, *14*, 281–295.

Hall, I. R., and C. I. Measures (1998), The distribution of Al in the IOC stations of the North Atlantic and Norwegian Sea between 52° and 65° North, *Mar. Chem.*, *61*, 69–85.

Hannan, J. R., H. E. Fuelberg, J. H. Crawford, G. W. Sachse, and D. R. Blake (2003), Role of wave cyclones in transporting boundary layer air to the free troposphere during the spring 2001 NASA/TRACE-P experiment, *J. Geophys. Res.*, *108*(D20), 8785, doi:10.1029/2002JD003105.

Hydes, D. J. (1989), Seasonal variations in dissolved aluminium concentrations in coastal waters and biological limitation of the export of the riverine input of aluminium to the deep sea, *Cont. Shelf Res.*, *9*(10), 919–929.

Lacan, F., and C. Jeandel (2004), Neodymium isotopic composition and rare earth element concentrations in the deep and intermediate Nordic Seas: Constraints on the Iceland Scotland Overflow Water signature, *Geochem. Geophys. Geosyst.*, *5*, Q11006, doi:10.1029/2004GC000742.

Landing, W. M., G. A. Cutter, J. A. Dalziel, A. R. Flegal, R. T. Powell, D. Schmidt, A. M. Shiller, P. Statham, S. Westerlund, and J. Resing (1995), Analytical intercomparison results from the 1990 Intergovernmental Oceanographic Commission Open-Ocean Baseline Survey for Trace Metals: Atlantic Ocean, *Mar. Chem.*, *49*, 253–265.

Liu, H., D. J. Jacob, I. Bey, R. M. Yantosca, B. N. Duncan, and G. W. Sachse (2003), Transport pathways for Asian pollution outflow over the Pacific: Interannual and seasonal variations, *J. Geophys. Res.*, *108*(D20), 8786, doi:10.1029/2002JD003102.

Martin, J. H., and S. E. Fitzwater (1988), Iron deficiency limits phytoplankton growth in the north-east Pacific subarctic, *Nature*, *331*, 341–343.

Measures, C. I. (1995), The distribution of Al in the IOC stations of the eastern Atlantic between 30°S and 34°N, *Mar. Chem.*, *49*, 267–281.

Measures, C. I., and E. T. Brown (1996), Estimating dust input to the Atlantic Ocean using surface water Al concentrations, in *The Impact of Desert Dust Across the Mediterranean*, edited by S. Guerzoni and R. Chester, pp. 301–311, Springer, New York.

Measures, C. I., and J. M. Edmond (1990), Aluminum in the South Atlantic: Steady state distribution of a short residence time element, *J. Geophys. Res.*, *95*(C4), 5331–5340.

Measures, C. I., B. Grant, M. Khadem, D. S. Lee, and J. M. Edmond (1984), Distribution of Be, Al, Se, and Bi in the surface waters of the western North Atlantic and Caribbean, *Earth Planet. Sci. Lett.*, *71*, 1–12.

Measures, C. I., M. T. Brown, and S. Vink (2005), Dust deposition to the surface waters of the western and central North Pacific inferred from surface water dissolved aluminum concentrations, *Geochem. Geophys. Geosyst.*, *6*, Q09M03, doi:10.1029/2005GC000922.

Measures, C. I., G. A. Cutter, W. M. Landing, and R. T. Powell (2006), Hydrographic observations during the 2002 IOC Contaminant Baseline Survey in the western Pacific Ocean, *Geochem. Geophys. Geosyst.*, *7*, Q03M06, doi:10.1029/2004GC000855.

Moran, S. B., and R. M. Moore (1988), Temporal variations in dissolved and particulate aluminum during a spring bloom, *Estuarine Coastal Shelf. Sci.*, *27*, 205–215.

Moran, S. B., and R. M. Moore (1991), The potential source of dissolved aluminum from resuspended sediments to the North Atlantic Deep Water, *Geochim. Cosmochim. Acta*, *55*, 2745–2751.

Ndung'u, K., J. R. Donat, M. Thomas, J. A. Consolvo, and A. R. Flegal (2001), Intercalibrated lead concentration measurements in the Atlantic Ocean, *Deep Sea Res., Part II*, *48*, 2781–2786.

Orians, K. J., and K. W. Bruland (1986), The biogeochemistry of aluminum in the Pacific Ocean, *Earth Planet. Sci. Lett.*, *78*, 397–410.

Orians, K. J., and K. W. Bruland (1988a), Dissolved gallium in the open ocean, *Nature*, *332*, 717–719.

Orians, K. J., and K. W. Bruland (1988b), The marine geochemistry of gallium: A comparison with dissolved aluminum, *Geochim. Cosmochim. Acta*, *52*, 2955–2962.

Peterson, R. G., and T. Whitworth (1989), The subantarctic and polar fronts in relation to deep water masses through the southwestern Atlantic, *J. Geophys. Res.*, *94*, 10,817–10,838.

Ranville, M. A., and A. R. Flegal (2005), Silver in the North Pacific Ocean, *Geochem. Geophys. Geosyst.*, *6*, Q03M01, doi:10.1029/2004GC000770.

Shiller, A. M. (1988), Enrichment of dissolved gallium relative to aluminum in natural waters, *Geochim. Cosmochim. Acta*, *52*, 1879–1882.

Shiller, A. M. (1998), Dissolved gallium in the Atlantic Ocean, *Mar. Chem.*, *61*, 87–99.

Suga, T., Y. Takei, and K. Hanawa (1997), Thermostad distribution in the North Pacific subtropical gyre: The general mode water and the subtropical mode water, *J. Phys. Oceanogr.*, *27*, 140–152.

Vink, S., and C. I. Measures (2001), The role of dust deposition in determining surface water distributions of Al and Fe in the south west Atlantic, *Deep Sea Res., Part II*, *48*, 2787–2809.

Vink, S., E. A. Boyle, C. I. Measures, and J. Yuan (2000), Automated high resolution determination of the trace elements iron and aluminum in the surface ocean using a towed fish coupled to flow injection analysis, *Deep Sea Res., Part I*, *47*, 1141–1156.

Wessel, P., and W. H. F. Smith (1998), New, improved version of Generic Mapping Tools released, *Eos Trans. AGU*, *79*(47), 579.

Wu, J., and E. A. Boyle (1997), Low blank preconcentration technique for the determination of lead, copper and cadmium in small-volume seawater samples by isotope dilution ICPMS, *Anal. Chem.*, *69*, 2464–2470.

Wu, J., and E. A. Boyle (1998), Determination of iron in seawater by high resolution isotope dilution inductively coupled plasma mass spectrometry after $Mg(OH)_2$ coprecipitation, *Anal. Chim. Acta*, *367*, 183–191.

You, Y. (2005), Unveiling the mystery of North Pacific Intermediate Water formation, *Eos Trans. AGU*, *86*, 65–71.